A Noninvasive Channel-Select Filter for a CMOS Bluetooth Receiver[1]

Alireza Zolfaghari and Behzad Razavi
Electrical Engineering Department
University of California, Los Angeles

Abstract

A fourth-order filter incorporates a method of suppressing interferers without filtering the desired signal, relaxing the trade-offs between noise, linearity, and power dissipation. Designed for the baseband of a 2.4-GHz receiver and fabricated in a 0.25 μm CMOS technology, the filter exhibits an input-referred noise of 17 nV/$\sqrt{\text{Hz}}$ while dissipating 2 mW from a 2.5-V supply and the receiver achieves a noise figure of 6 dB with a power consumption of 17.5 mW.

I. Introduction

Analog filters used in the baseband section of RF receivers must satisfy stringent noise, linearity, power dissipation, and selectivity requirements. The existence of large interferers near the desired signal frequency demands a high linearity and/or low noise in the filters, impacting the distribution of gain and noise through the receiver chain. This paper describes a "noninvasive" filtering technique that substantially relaxes the trade-offs between the above parameters. The technique can be exploited in both discrete-time and continuous-time implementations and its merits are demonstrated in a g_m-C prototype designed for a 2.4-GHz RF CMOS receiver for Bluetooth.

II. Filter Environment and Concept

Figure 1 shows the transceiver architecture [1]. The receiver

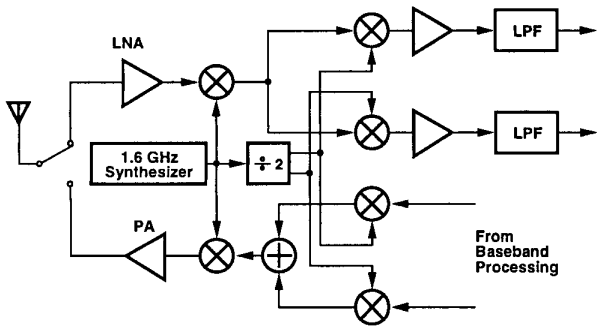

Fig. 1. Transceiver architecture.

employs two downconversion stages using a first local oscillator (LO) frequency of 1.6 GHz and a second LO frequency of 800 MHz, translating the input spectrum from 2.4 GHz to an intermediate frequency (IF) of 800 MHz and subsequently to zero. The baseband signals are then applied to channel-select low-pass filters (LPF's). The RF building blocks were presented in [1] and in this paper we focus on the design and implementation of the channel-select filters using a noninvasive technique.

The conventional approach to filtering requires that both the signal and the interferers travel through a circuit that provides the desired transfer function [Fig. 2(a)]. However, such a filter introduces significant noise and intermodulation in the signal band. It is therefore advantageous to seek a method that applies filtering to only interferers without "invading" the signal band. For example, as illustrated in Fig. 2(b), a complex impedance

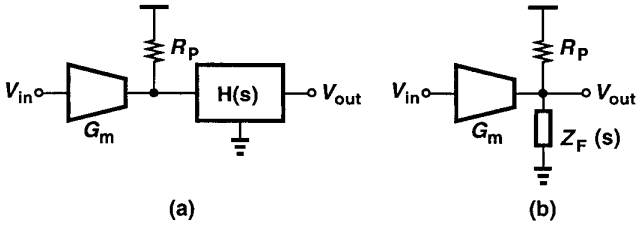

Fig. 2. (a) Conventional filtering (b) noninvasive filtering.

$Z_F(s)$ can be placed in parallel with the signal path such that it operates as an open in the signal band while shunting the interferers to ground. As a result, $Z_F(s)$ provides selectivity with negligible additional noise, a critical advantage in view of the high $1/f$ corner frequency in modern CMOS devices. Furthermore, $Z_F(s)$ creates a small intermodulation current through R_P because its Thevenin equivalent is relatively high in the signal band. Nevertheless, some linearity is still necessary if $Z_F(s)$ is to operate as an effective shunt at interferer frequencies.

III. Filter Topology

The implementation of one section is shown in Fig. 3 in a single-ended form. Here, $Z_F(s)$ consists of an integrator loaded by an emulated inductor $L_L = C_L/(G_{m2}G_{m3})$. The transfer function is given by

[1]This work was supported in part by Conexant.

0-7803-7250-6/02/$10.00 © 2002 IEEE

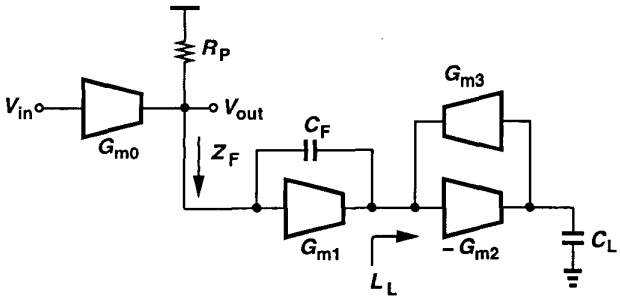

Fig. 3. Second-order noninvasive filter topology.

$$\frac{V_{out}}{V_{in}}(s) = G_{m0}R_P \cdot \frac{1 + \frac{C_F C_L}{G_{m2}G_{m3}}s^2}{1 + R_P C_F s + \frac{C_F C_L}{G_{m2}G_{m3}}(R_P G_{m1} + 1)s^2}. \quad (1)$$

The zero results from the resonance of C_F with L_L and can be chosen to create a deep notch in the adjacent channel.

The noise performance of the circuit is revealed by the following equation:

$$\overline{v_{n,G_m}^2} = 4kT\Gamma R_P^2\left(\frac{C_F C_L}{G_{m2}G_{m3}}\right)^2 \cdot \frac{\omega^2[\omega^2(G_{m1} + G_{m3}) + \frac{G_{m3}^2 G_{m1}}{C_L^2}]}{[1 - \frac{C_F C_L}{G_{m2}G_{m3}}(R_P G_{m1} + 1)^2\omega^2]^2 + R_P^2 C_F^2 \omega^2}, \quad (2)$$

where the noise of each transconductor is expressed as $4kTG_m\Gamma$ and only the noise of G_{m1}-G_{m3} is included. This transfer function exhibits the same poles as (1), but as expected, it also provides a zero at DC, thereby suppressing the effect of flicker noise. The other zero is typically higher than the poles, resulting in the noise shaping function shown in Fig. 4. The key observation is that the area under this plot

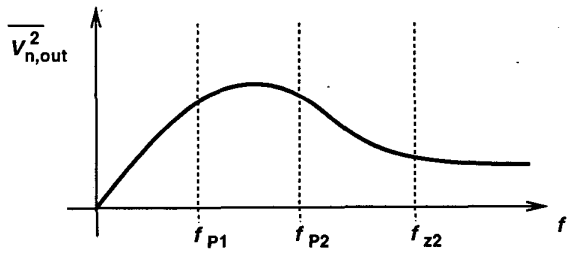

Fig. 4. Output noise of the filter produced by transconductor stages.

is typically much less than the noise contributed by G_{m0} and R_P.

The topology of Fig. 3 may prove inadequate in some applications. In an RF receiver, for example, the circuit may not provide enough rejection beyond the signal channel and the adjacent channel. This issue can be resolved by increasing the order of $Z_F(s)$ or using cascaded biquad sections as shown in Fig. 5.

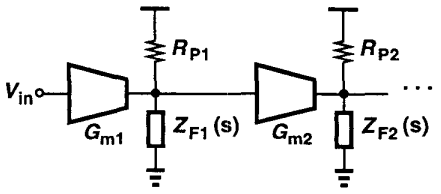

Fig. 5. Higher order noninvasive filtering.

IV. Filter Design

The filter designed here serves to suppress interferers in a Bluetooth receiver. Illustrated in Fig. 6, scenarios where the filter selectivity becomes critical include (a) an adjacent channel interferer as strong as the signal; (b) an alternate channel interferer 30 dB higher than the signal; (c) a second alternate interferer 40 dB higher than the signal. With 40 dB of receiver

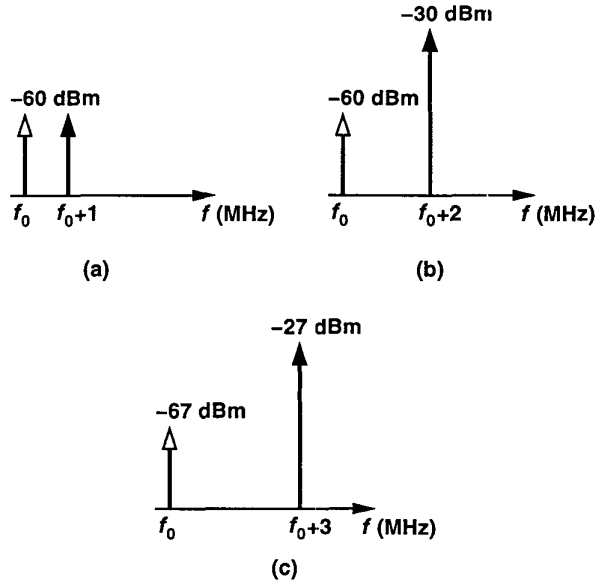

Fig. 6. Interferers (black arrows) and the desired signal(white arrow) levels in Bluetooth.

gain preceding the filter, the interferers applied to the filter exhibit large amplitudes, requiring a high linearity. To determine the maximum tolerable noise and nonlinearity of the filter as well as its minimum order, a Matlab program was written that includes a GFSK detector and hence a means of calculating the bit error rate. This study indicates that a cascade of two second-order sections yields sufficient selectivity if they introduce deep notches in the adjacent channels. To achieve the selectivity required for Bluetooth, the overall filter consists of two cascaded sections, one yielding a notch at 1 MHz and the other at 3 MHz to suppress the adjacent channels. Note that a fourth-order elliptic reallization achieves comparable suppression but at the cost of greater sensitivity to the element values. For this reason, cascaded biquads are preferred

V. Filter Realization

With four transconductors per section, the filter can potentially consume a high power. Figure 7 depicts a low-power, tunable implementation of the transconductor, where

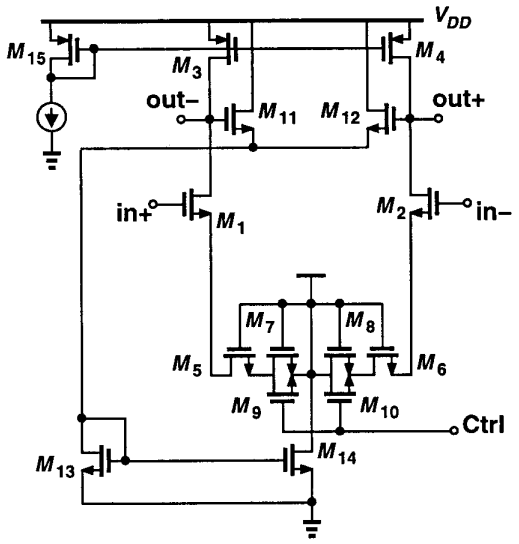

Fig. 7. Transconductor circuit.

the amount of degeneration is partially controlled by varying the on-resistance of M_9 and M_{10}. With their gates tied to V_{DD}, M_7 and M_8 "soften" the variation as the control voltage falls. This topology is used for G_{m1}-G_{m3} in Fig. 3. Each transconductor consumes 34 μW to provide a transconductance of 25 $\mu\Omega^{-1}$. As with conventional filters, the prototype can be tuned using a phase-locked loop.

The implementation of the filter in a digital technology mandates a MOS realization for R_P in Fig. 3. To achieve process and temperature tracking, G_{m0} and R_P are designed as shown in Fig. 8. Here, diode-connected transistors M_1-M_2 and triode devices M_5-M_{10} form the load resistor and are tuned along with the other transconductors. Note that, as predicted by Eq. (1), the transconductance of this circuit does not affect the shape of the transfer function. This suggests the possibility of using them as a variable-gain amplifier in the receiver.

The lack of high-density, linear capacitors in this technology makes the implementation of C_F and C_L in Fig. 3 difficult. In particular, with a cut-off frequency of 400 kHz and two second-order sections, the filter demands a total capacitance of approximately 100 pF, which translates to a large area even for lateral flux capacitors. This is overcome through the use of back-to-back PMOS devices as shown in Fig. 9. Here, the gates of the devices are connected to ground through an n-well resistor so as to ensure operation in strong inversion. The value of R_G must be high enough to affect the transfer function negligibly. Figure 10 plots the overall filter transfer function for different values of R_G, indicating that R_G $\approx$500 kΩ is adequate.

Figure 11 shows the simulated output noise of the filter. Simulation results also indicate that the output noise generated

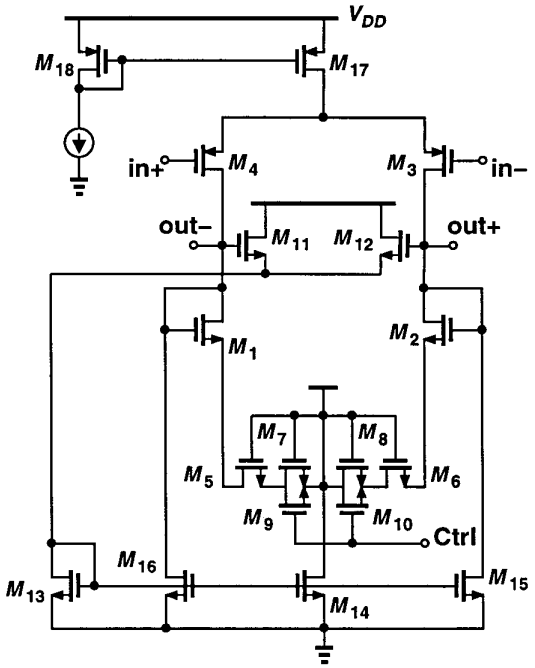

Fig. 8. Input transconductor and parallel resistor.

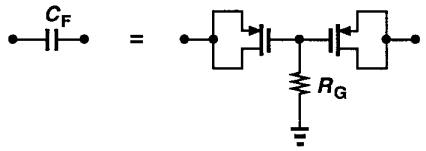

Fig. 9. Floating capacitors realized by back-to-back PMOS devices.

by the input transconductors (G_{m0}'s) and parallel resistors (R_P's) is 147 nV/$\sqrt{Hz}$. This confirms that the noninvasive filters introduce no noise at dc and contribute negligible noise across the passband.

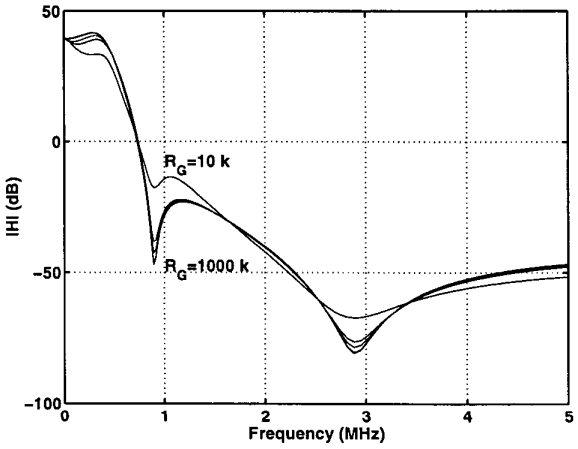

Fig. 10. Simulated filter characteristic for R_G =10, 50, 100, 500, and 1000 kΩ.

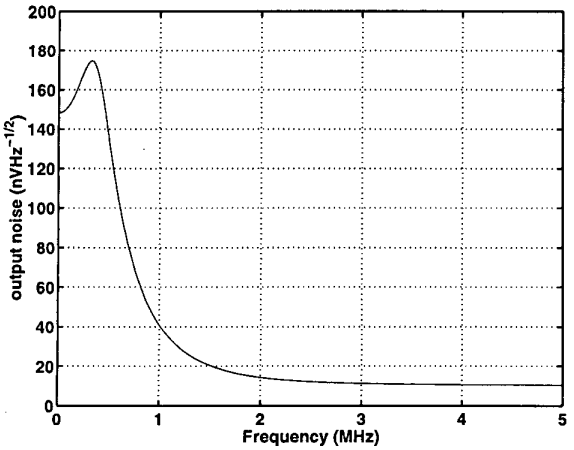

Fig. 11. Simulated output noise of the noninvasive filters.

VI. Experimental Results

The transceiver has been fabricated in a 0.25-μm digital CMOS technology. The die photo is shown Fig. 12, where

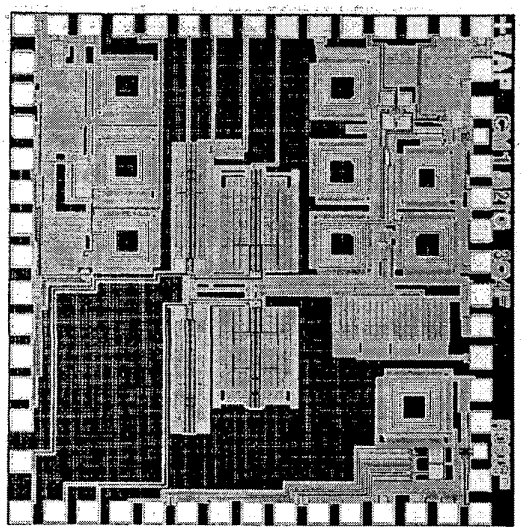

Fig. 12. Transceiver die photograph.

each filter occupies an area of approximately 0.5×0.5 mm^2. Table 1 summarizes the measured performance of the receiver. The overall system is tested with a 2.5-V supply. Figure 13 shows the receiver transfer characteristics, displaying deep notches around 1 MHz and 3 MHz.

The noise figure of the receiver is 6 dB at 200 kHz, a value close to simulated results. Assuming a signal-to-noise ratio of 20 dB required to detect the baseband signal, this translates into a sensitivity of -88 dBm. With the measured gain, the in-band noise of the noninvasive filter is calculated to be 17 nV/$\sqrt{\text{Hz}}$. The power dissipation of each filter is 2 mW and the total power dissipation of the receiver is 17.5 mW.

The linearity of the filter is measured by applying two interferers of magnitude -39 dBm (at the input of the receiver), in the third and sixth adjacent channels. The signal-to-intermodulation ratio is 26 dB, well above the level required for the specified bit error rate.

Noise Figure	6 dB
$\lvert S_{11}\rvert$	-12 dB
Image Rejection	41 dB
Voltage Gain	50 dB
Signal/IM	26 dB
Technology	0.25-μm CMOS
Die Area	1.83×2mm^2
Supply Voltage	2.5 V
Power Dissipation:	
LNA and Mixers	6.25 mW
Divider	3.75 mW
Baseband Amplifiers	3.5 mW
I and Q LPF's	4 mW
Total	17.5 mW

Table 1. Measured receiver performance.

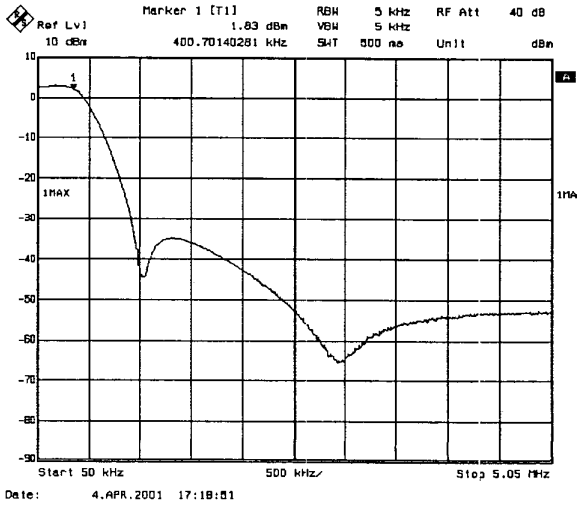

Fig. 13. Measured receiver characteristic.

The low-power techniques employed in the transceiver and in particular the I and Q baseband filters result in an overall power dissipation that is a factor of five lower than that of prior art [3]. In addition, the receiver achieves 8 dB better sensitivity than that in [3].

References

[1] A. Zolfaghari, A. Chan, and B. Razavi "A 2.4 GHz 34mW CMOS Transceiver for Frequency-Hopping and Direct-Sequence Applications," *ISSCC Dig. of Tech. Papers*, pp. 418-419, Feb. 2001.

[2] B. Nauta *Analog CMOS Filters for Very High Frequencies* Kluwer Academic Publishers, 1993.

[3] H. Darabi *et al.*, "A 2.4GHz CMOS Transceiver for Bluetooth," *ISSCC Dig. of Tech. Papers*, pp. 200-201, Feb. 2001.